JOURNAL OF SPACECRAFT AND ROCKETS
Vol. 31, No. 5, September–October 1994

Cadmium Simulation of Orbital-Debris Shield Performance to Scaled Velocities of 18 km/s

Robert M. Schmidt* and Kevin R. Housen†
Boeing Defense & Space Group, Seattle, Washington 98124
and
Andrew J. Piekutowski‡ and Kevin L. Poormon§
University of Dayton Research Institute, Dayton, Ohio 45469

An experimental technique is developed and used to simulate the response of aluminum debris shields for impacts up to 18 km/s. To simulate an aluminum impact on an aluminum shield, the velocity is reduced by a scale factor, and the impactor and bumper are surrogates that have the same dimensions as the originals, but are composed of a material whose specific energies of melting and vaporization are much lower than those of aluminum. Cadmium is used as the surrogate material, because it has unique properties that satisfy the attendant scaling requirements and because its velocity scale factor is 3.1, thereby allowing tests at actual velocities up to 5.8 km/s to simulate aluminum impacts at velocities up to 18 km/s. Such tests reproduce the initial momentum of an aluminum impactor and the impulse distribution delivered to the rear wall. Cadmium tests, at scaled velocities near 7 km/s, agreed well with aluminum tests near 7 km/s, both in terms of debris cloud geometry and the minimum impactor size for wall perforation. Simulations at higher scaled velocities showed that the minimum diameter for penetration increases with increasing velocities above 10.5 km/s, in sharp contrast to current empirical shield models.

Nomenclature

b = thickness of bumper
D = diameter of wall area affected by debris cloud
d = diameter of impactor
F = resisting force
f = functional dependence
H_b = energy per unit mass for vaporization of bumper
H_i = energy per unit mass for vaporization of impactor
h_b = energy per unit mass for melting of bumper
h_i = energy per unit mass for melting of impactor
I = momentum per unit area delivered by debris cloud to wall
I^* = threshold momentum per unit area for wall failure
M = mass of debris cloud and wall material it impacts
m_c = mass of debris cloud
S = spacing between bumper and wall
t = thickness of wall
U = impactor velocity
v = initial velocity imparted to wall
v_c = average axial velocity of debris cloud
Y_b = strength measure for bumper
Y_i = strength measure for impactor
Y_w = strength measure for wall
β = density of bumper material
Δ = deflection of wall along axis of impact
Δ^* = threshold wall deflection at which failure occurs
δ = density of impactor material
ϵ = strain measure for wall failure
ρ = density of wall material
τ = time required to complete wall deflection

Received Jan. 5, 1993; revision received Nov. 5, 1993; accepted for publication Nov. 22, 1993.

*Technical Fellow.
†Principal Engineer.
‡Senior Research Engineer.
§Associate Research Engineer.

Introduction

CONVENTIONAL launch techniques are limited to velocities of 7.5 km/s or less. In this low-velocity regime, where vaporization of aluminum is insignificant, the effectiveness of a debris shield rests on its ability to fragment and/or melt an impacting particle. This regime has been studied experimentally in detail. On the other hand, as the velocity increases above 7 km/s, the physical mechanisms involved in shield penetration change, because partial or total vaporization of aluminum can occur. Consequently, experimental results at 7 km/s and slower cannot be simply scaled or extrapolated in an ad hoc manner to predict results for higher-speed impacts. This is important, because current estimates of the orbital debris environment[1] indicate that most debris impacts occur in excess of 7 km/s.

To investigate the high-velocity response of aluminum shields, a simulation technique was developed using cadmium as a substitute material, because it melts and vaporizes at much lower specific energies than aluminum. Cadmium has been used by various investigators[2–7] to visualize and investigate debris cloud behavior for impacts undergoing melt and vaporization. Hopkins et al.[5] reported experiments using a single aluminum or cadmium bumper placed in front of a 6061-T6 aluminum wall. The impactor and bumper were composed of identical materials. They varied the wall thickness, while holding the bumper thickness (0.81 mm), wall-to-bumper spacing (50.8 mm), and impactor diameter (3.18 mm) constant, to determine the minimum wall thickness necessary to avoid perforation as a function of impact velocity. Although no attempt was made to infer the debris shield's effectiveness for aluminum in the vaporization regime, their data showed some interesting qualitative features. Figure 1 reproduces the results of Hopkins et al. for aluminum and cadmium. As the impact velocity is increased, the wall thickness required to prevent perforation might be expected to increase. The aluminum curve does show this trend, except for velocity intervals following the onset of impactor fragmentation near 3 km/s and melting at about 5.5 km/s. In these intervals the curve slopes downward, because the effect of fragmentation or melting is to distribute the loading more uniformly over the wall. The aluminum curve shows an upward turn at 7 km/s, as do many models of shield failure,[8–10] which predict that the curve should continue upward for velocities beyond 7 km/s.

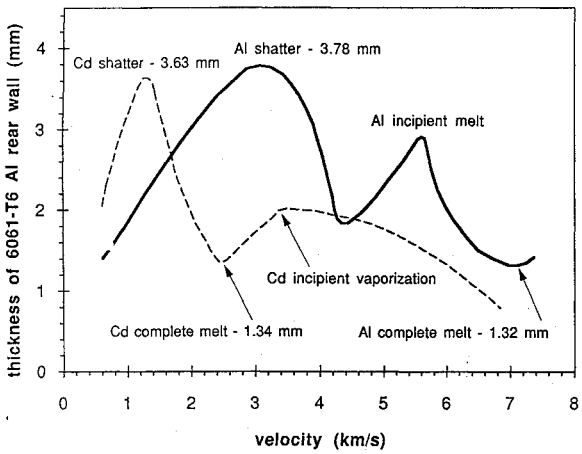

Fig. 1 Minimum wall thickness that did not perforate, as a function of velocity. Results are for aluminum-on-aluminum and cadmium-on-cadmium impacts with identical geometry for the impactor, bumper, and spacing.

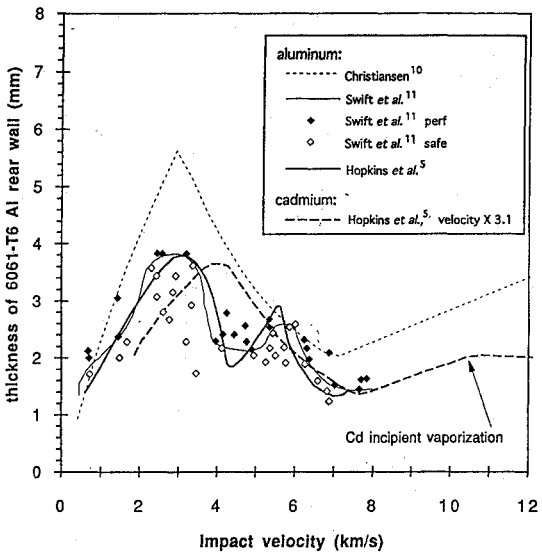

Fig. 2 Cadmium data from Hopkins et al.[5] scaled by a multiplicative factor of 3.1 in velocity, based on phase-transition specific energies. Aluminum data points are from Swift et al.[11]

The cadmium results show features qualitatively similar to those for aluminum, but at correspondingly lower velocities, because the strength and the specific energy required for melting are lower for cadmium. Although the cadmium data do not show an intermediate peak at incipient melting, they do reproduce the fragmentation peak and a local minimum in the curve at complete melting, and show respective wall thicknesses that are nearly identical to those for aluminum.

The similarity between the two data sets at or below the point of complete melting can be emphasized by using an empirical factor of 3.1 to scale the impact velocity of the cadmium to an equivalent velocity for an aluminum target. As shown in Fig. 2, this produces good agreement at the minimum where melting occurs, with less agreement in the fragmentation regime. Because of threefold velocity scale compression, the incipient-melting peak may have been missed for the cadmium curve (the actual data points from the tests of Hopkins et al.[5] were never published). The most interesting feature of the cadmium tests is the behavior above 2.5 km/s, which corresponds to the region above 7 km/s on the aluminum curve. The cadmium curve slopes upward, in agreement with model predictions for aluminum above 7 km/s. However, at the point where vaporization initiates, the cadmium curve turns downward, in sharp contrast to predictions of current shield models.

Figure 2 also shows a model prediction from Christiansen,[10] which has the same qualitative trend as the scaled cadmium data, up to a velocity of about 10.5 km/s. However, at higher velocities the cadmium curve levels off and turns down (see Fig. 1). This observation, together with the agreement between the aluminum and scaled cadmium data of Hopkins et al.[5] shown in Fig. 2, provided the impetus for the present study. A preliminary series of experiments was designed specifically to test the fidelity of cadmium simulations and to explore the high-velocity regime. In contrast to the variable-wall-thickness configuration used by Hopkins et al.,[5] the present tests used fixed dimensions for the bumper, wall, and spacing and varied the impactor to find the minimum diameter that would cause perforation at a variety of impact velocities. In the next section, dimensional analysis and a model of wall failure are used to develop the rationale and similarity requirements necessary to scale cadmium tests to equivalent impacts on an aluminum bumper.

Scaling of Debris-Shield Experiments

The impact of a sphere onto a standard Whipple shield, as defined in Fig. 3, is assumed to occur along an axis normal to the bumper. As the impactor penetrates the bumper, a debris cloud is formed, whose characteristics depend on the variables listed in Fig. 3. A model is developed below that shows for impact velocities sufficiently large that the debris cloud consists mostly of melted and/or vaporized material, the wall fails if the specific impulse I (impulse/area) delivered to the wall exceeds a threshold value. This provides the basis for the proposed simulation technique. A prototype impact event, in which an aluminum particle strikes an aluminum bumper at a given velocity, is simulated by a slower impact in which the impactor and bumper materials are replaced by surrogates. The surrogate materials and the impact velocity in the simulation are chosen in such a way that the specific impulse of the debris cloud is the same as in the prototype event. That is, the simulation delivers the same impulsive loading to the wall as the prototype.

For the case considered here, i.e., aluminum impacts at normal incidence, the debris cloud consists largely of molten or vaporized material if the impact velocity is greater than $\sim$ 7 km/s (see Fig. 1). Therefore, the use of specific impulse in the development of shield scaling laws is expected to hold only for this velocity regime. However, as noted in the next section, there is some evidence that the scaling laws may apply to aluminum-impact velocities as low as 4 km/s.

The specific impulse delivered by the debris cloud is written in terms of the variables that describe the impactor, those that describe the bumper, and the spacing, viz.,

$$I = f[U, d, \delta, Y_i, h_i, H_i, \quad b, \beta, Y_b, h_b, H_b, \quad S] \tag{1}$$

There are three independent dimensional units involved in Eq. (1). Therefore, dimensional analysis allows this equation to be written in terms of three fewer variables by expressing them in nondimensional form, i.e.,

$$\frac{IS^2}{\delta b^3\sqrt{h_i}} = f\left[\frac{U}{\sqrt{h_i}}, \frac{d}{b}, \frac{Y_i}{\delta h_i}, \frac{h_i}{H_i}, \frac{\beta}{\delta}, \frac{Y_b}{Y_i}, \frac{h_b}{h_i}, \frac{H_b}{H_i}, \frac{S}{b}\right] \tag{2}$$

so that I is given by

$$I = \frac{\delta b^3\sqrt{h_i}}{S^2} f\left[\frac{U}{\sqrt{h_i}}, \frac{d}{b}, \frac{Y_i}{\delta h_i}, \frac{h_i}{H_i}, \frac{\beta}{\delta}, \frac{Y_b}{Y_i}, \frac{h_b}{h_i}, \frac{H_b}{H_i}, \frac{S}{b}\right] \tag{3}$$

The specific impulse in the simulation matches that of the prototype if the terms on the right side of Eq. (3) are held constant. There are various ways to achieve this similarity. As a practical expedient, the following conditions are adopted: the impactor is composed of the same material as the bumper, and the length scales d, b, and S in the simulation are the same as in the prototype. That is, the simulation uses a geometric replica of the prototype shield. Under these conditions, d, b, S, and the ratios β/δ, Y_b/Y_i, h_b/h_i, and H_b/H_i are all constant. Therefore, Eq. (3) becomes

$$I = \delta\sqrt{h_i} f\left[\frac{U}{\sqrt{h_i}}, \frac{Y_i}{\delta h_i}, \frac{h_i}{H_i}\right] \tag{4}$$

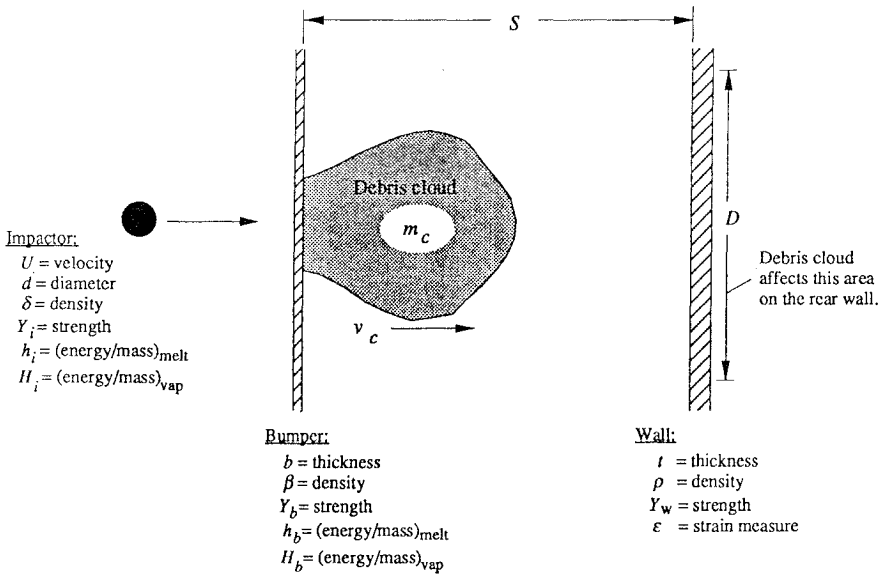

Fig. 3 Definition of variables used in Whipple-shield scaling analysis.

In the simulation, the values for the remaining four terms on the right side of Eq. (4) must equal the values for the prototype event. Although an exact match is impossible, cadmium provides the best match of any known material. The similarity requirements, based on Eq. (4), together with the actual conditions attained for cadmium are as follows:

	Similarity requirement	Actual ratio	
scaled velocity:	$\frac{U}{\sqrt{h_i}} = \text{constant}$		
	$\Rightarrow \frac{U_{Cd}}{U_{Al}}\sqrt{\frac{h_{i,Al}}{h_{i,Cd}}} = 1$	1.0	(5)
total momentum:	$\delta\sqrt{h_i} = \text{constant}$		
	$\Rightarrow \frac{\delta_{Cd}}{\delta_{Al}}\sqrt{\frac{h_{i,Cd}}{h_{i,Al}}} = 1$	1.0	(6)
ratio of specific heats:	$\frac{h_i}{H_i} = \text{constant}$		
	$\Rightarrow \frac{H_{i,Al}}{H_{i,Cd}}\frac{h_{i,Cd}}{h_{i,Al}} = 1$	1.2	(7)
scaled strength:	$\frac{Y_i}{\delta h_i} = \text{constant}$		
	$\Rightarrow \frac{Y_{i,Cd}}{Y_{i,Al}}\frac{[\delta h_i]_{Al}}{[\delta h_i]_{Cd}} = 1$	1.1 ± 0.4	(8)

The impact velocity in a cadmium simulation is chosen to satisfy the requirement given in Eq. (5). Holsapple[12] considered various energy measures for melting in impacts of aluminum on aluminum and cadmium on cadmium. He showed that $\sqrt{h_{i,Al}/h_{i,Cd}}$ has a value of 3.2 under the conditions that some melting occurs as the shocked material unloads, and a value of 3.0 under the condition of complete melting on unloading. A value of 3.1 is adopted here because it is intermediate to the values calculated by Holsapple and because it provides a good correlation of the results of Hopkins et al. discussed above and shown in Fig. 2. Therefore, to simulate an aluminum impact at velocity U, the cadmium impact is performed at a reduced velocity of $U/3.1$. As a result, aluminum impacts at velocities up to 21.7 km/s can be simulated by launching cadmium at velocities up to 7 km/s.

Note that the velocity scale factor could also be determined from the static properties of cadmium and aluminum. The static values reported by Holsapple[12] give a scale factor of 2.9. Note that static properties apply only to isobaric conditions. Although these properties may be important in determining the final state of the material in the debris cloud, they are less relevant to the mechanisms of interest here, which occur over a wide range of pressures and on short time scales (e.g., the transit time for the cloud to reach the wall is of order 100 μs).

Equation (6) is a requirement that the impactor momentum be the same in the simulation as in the prototype (because the impactor size is held constant and, from Eq. [5], the impact velocity is proportional to $\sqrt{h_i}$). The ratio of the density of pure cadmium to that of 2017-T4 aluminum is $8.65/2.79 = 3.1$. The square root of the ratio of the heats of melting is 1/3.1, as noted above. Therefore, the ratio shown in Eq. (6) is $3.1/3.1 = 1.0$.

Holsapple[12] also considered energy measures for vaporization. The ratio $H_{i,Al}/H_{i,Cd}$, under the condition that some vaporization occurs on unloading, was found to be 11.8. The same condition for melting gave $h_{i,Cd}/h_{i,Al} = 1/10.0$. Therefore the ratio shown in Eq. (7) is $11.8/10.0 = 1.2$.

The similarity condition given in Eq. (8) is evaluated by using handbook values of the strength of aluminum and cadmium. The ultimate tensile strength of 2017-T4 aluminum is 4.3 kbar,[13] while that of pure cadmium varies over a range of 1 to 2 kbar,[14] depending on the degree of cold work. Recalling that the density ratio δ_{Al}/δ_{Cd} is 1/3.1 and the ratio $h_{i,Al}/h_{i,Cd}$ is 10.0, the ratio shown in Eq. (8) is $[(1.5 \pm 0.5)/4.3](1/3.1)10.0 = 1.1 \pm 0.4$.

Therefore, cadmium is a good surrogate for aluminum, based on the similarity requirements discussed above. Of course, it is not known in advance how sensitive the outcome of an impact event is to the various parameters. For example, if the specific impulse is insensitive to the impactor strength, then a ratio significantly different from unity in Eq. (8) might have only a small effect on the outcome of an impact event.

Mullin et al.[7] reported data that support the use of cadmium as a surrogate for aluminum. They measured debris cloud momentum transferred to a ballistic pendulum for impacts using aluminum, cadmium, and zinc, where the impactor and bumper were composed of a common material. The impact velocity was varied while holding the bumper thickness, spacing, and impactor diameter constant. These initial conditions are identical to those that led to Eq. (4). A plot of $I/(\delta\sqrt{h_i})$ vs $U/\sqrt{h_i}$ shows their data for aluminum, cadmium, and zinc all fall on a common curve. This indicates that either the similarity requirements listed in Eqs. (6), (7), and (8) are satisfied when using cadmium [and possibly zinc, although geometric similarity of the shield cannot be attained for zinc, namely, Eq. (6) does not hold for zinc] as a simulant of aluminum, or the momentum imparted to the wall is insensitive to small violations of the requirements. In either case, these data confirm that cadmium reproduces the momentum delivered by an aluminum impact.

The assumption that wall failure occurs when the specific impulse exceeds a threshold value is based on the following model of wall failure, which, although simple, captures the essential physical mechanisms involved. An impactor strikes the bumper, producing a cloud of debris that consists of both impactor and bumper material. Denoting the mass and average axial velocity of the cloud as m_c and v_c, respectively, and assuming that the collision of the cloud with the wall is perfectly inelastic (an elastic case is considered below), the wall is given an initial axial velocity

$$v = (m_c/M)v_c \tag{9}$$

where M is the sum of m_c and the mass of the portion of the wall that is given the initial velocity v.

If the affected area of the wall has diameter D, then $M = m_c + \pi D^2 \rho t/4$. The impulsive loading results in bulging of the wall, with a final displacement Δ along the axis of the impact. The outward movement of the wall is assumed to be impeded by a constant resisting force F, and therefore a constant deceleration F/M. The distension of the wall stops after a time $\tau = vM/F$. The final displacement is found from

$$\Delta = v\tau - 1/2(F/M)\tau^2 = (Mv^2/2F) \tag{10}$$

Taking the resisting force F to be proportional to $Y_w Dt$ and substituting for M and v, Eq. (10) becomes

$$\Delta \propto \frac{m_c^2 v_c^2}{t^2 Y_w \rho D^3 (1 + 4m_c/\pi D^2 \rho t)} \tag{11}$$

For the cases of interest here, the factor $1 + 4m_c/(\pi D^2 \rho t)$ is very close to 1. Noting that the specific impulse I delivered to the wall is $4m_c v_c/(\pi D^2)$, Eq. (11) becomes

$$\Delta \propto \frac{I^2 D}{t^2 Y_w \rho} \tag{12}$$

Failure of the wall occurs when Δ exceeds a threshold value Δ^*, which is proportional to $D\varepsilon$. Therefore, substituting $D\varepsilon$ for Δ in Eq. (12), failure is found to occur when the specific impulse exceeds a threshold value I^* given by

$$I^* \propto t\sqrt{\rho Y_w \varepsilon} \tag{13}$$

Equation (13) justifies the statement made at the beginning of this section that failure occurs when the momentum per unit area delivered to the wall exceeds a critical value.

The derivation of Eq. (13) assumed that the interaction of the debris cloud with the wall is perfectly inelastic. This is not a crucial assumption. For example, if the interaction is assumed to be perfectly elastic, Eq. (11) is altered by only a factor of $\sqrt{1 + 4m_c/\pi D^2 \rho t}$, which, as noted above, is very close to 1, because the mass of the wall material affected is much larger than the mass of the debris cloud. Therefore, Eq. (13) is obtained regardless of whether the interaction with the wall is elastic, inelastic, or some combination thereof.

The minimum impactor diameter required for wall failure is found by replacing I^* in Eq. (13) by I given in Eq. (3), with an additional simplification. For two experiments identical in every way except for the spacing S, the momentum per unit area delivered to the wall is expected to be proportional to S^{-2}. This follows directly from the observations discussed below that cloud expansion is very nearly isotropic. That is, if S is increased by a factor of 2, all linear dimensions of a cloud increase by a factor of 2 by the time the cloud encounters the wall. Hence, the affected area of the wall increases by a factor of 4, and the impulse per unit area decreases by the same factor. The first term on the right side of Eq. (3) shows this expected dependence on S, indicating that no further dependence on S is required. Therefore, the argument S/b is dropped from the right side of Eq. (3). Equating I in Eq. (3) to I^* in Eq. (13) gives

$$\frac{tS^2}{\delta b^3}\sqrt{\frac{\rho Y_w \varepsilon}{h_i}} = f\left[\frac{U}{\sqrt{h_i}}, \frac{d}{b}, \frac{Y_i}{\delta h_i}, \frac{h_i}{H_i}, \frac{\beta}{\delta}, \frac{Y_b}{Y_i}, \frac{h_b}{h_i}, \frac{H_b}{H_i}\right] \tag{14}$$

which is rearranged to give the minimum impactor diameter required for failure of the wall, i.e.,

$$\frac{d}{b} = f\left[\frac{U}{\sqrt{h_i}}, \frac{tS^2}{\delta b^3}\sqrt{\frac{\rho Y_w \varepsilon}{h_i}}, \frac{Y_i}{\delta h_i}, \frac{h_i}{H_i}, \frac{\beta}{\delta}, \frac{Y_b}{Y_i}, \frac{h_b}{h_i}, \frac{H_b}{H_i}\right] \tag{15}$$

Note that the assumption $I \propto S^2$ probably does not hold for impactors that are distinctly nonspherical. For example, as discussed below, a disk-shaped projectile impacting flat against a bumper produces a cloud whose radial dispersion with distance is negligible. In the limiting case in which the cloud shows no radial expansion as it propagates, the function on the right side of Eq. (3) is expected to be proportional to $(S/b)^2$, so that I would be independent of S. The scaling equation that results from such an assumption is identical to Eq. (15), except that the factor S^2/b^3 on the right side of Eq. (15) is replaced by $1/b$.

Returning to the case of spherical impactors, when an aluminum impact on an aluminum bumper is simulated with cadmium, the last six arguments on the right side of Eq. (15) are constant, as discussed above. Therefore, the minimum impactor diameter is given by

$$\frac{d}{b} = f\left[\frac{U}{\sqrt{h_i}}, \frac{tS^2}{\delta b^3}\sqrt{\frac{\rho Y_w \varepsilon}{H_i}}\right] \tag{16}$$

Additionally, if the cadmium simulation employs the same wall material and thickness, bumper thickness, and spacing as the aluminum prototype, Eq. (16) reduces to

$$d = f(U/\sqrt{h_i}) \tag{17}$$

Therefore, if the scaled velocity $U/\sqrt{h_i}$ is held constant, the minimum impactor diameter for wall failure in the cadmium simulation is identical to that for the aluminum prototype.

Equation (17) provides the basis for determining the ballistic limit of an aluminum debris shield for impact velocities above 7 km/s. For example, the minimum impactor diameter required to perforate the wall of a debris shield at, say, 12 km/s is determined by replacing the impactor and bumper with cadmium and performing tests at a velocity of 12/3.1 = 3.87 km/s. Experiments using this simulation technique are described in the following sections.

Description of Experiments

The tests reported here were conducted at the University of Dayton Research Institute (UDRI). A description of the facility and the experimental techniques involved is provided by Piekutowski.[15–17] Table 1 summarizes the initial conditions and results of these tests.

A series of hypervelocity impact tests was performed to validate the use of cadmium in the simulation technique discussed above. To accomplish this with a limited number of tests, the impactor velocity and size were varied while, for the most part, all other shield parameters were held constant. The nominal shield configuration of interest was a 1.27-mm-thick (50-mil) bumper placed 101.6 mm (4 in.) in front of a 3.18-mm-thick ($\frac{1}{8}$-in.) 2219-T87 aluminum wall. This configuration was chosen because considerable data are available for aluminum impacts.[18,19] The walls were square, nominally 406 mm (16 in.) on a side, and were supported at their corners. The impactors were spherical and struck the bumpers at an incidence angle of 90 deg (i.e., normal to the bumper), except as noted in Table 1. Flash x-rays were used to confirm the integrity and sphericity of the impactor prior to impact. These ballistic limit tests did not provide much information on the evolution of the debris cloud, because the placement of the wall allowed only a single x-ray image of the debris cloud per shot. Therefore, several tests were conducted with the wall placed at spacings up to 380 mm (15 in.), allowing up to three consecutive images of the cloud to be obtained.

Lastly, three shots were dedicated to investigating shape effects peculiar to thin-disk projectiles. The results were compared with the hypervelocity-launcher (HVL) data reported by Ang et al.[20] and Hill et al.[21]

Table 1 Summary of experimental results.

Shot number	Impactor mass m, g	Impactor diameter d, mm	Impactor velocity U, km/s	Scaled velocity, km/s	Bumper thickness b, mm	Bumper material	Bumper hole diam mm	Bumper spacing S, mm	Wall thickness t, mm	Wall material	Wall size mm × mm	Wall failure	Wall bulge Δ, mm	Wall hole diam, mm	Wall crack size, mm
4-1403	1.175	6.38	5.78	17.9	1.27	Cadmium	15.6	102	3.18	2219-T87	229 × 229	No	11.8	—	—
4-1404	1.160	6.35	2.26	7.0	1.27	Cadmium	11.7	102	3.18	2219-T87	229 × 229	Yes	9.2	6.4	30.5
4-1405	1.156	6.34	3.48	10.8	1.27	Cadmium	14.0	102	3.18	2219-T87	406 × 406	Yes	10.5	7.1	71.1
4-1406	1.171	6.37	2.47	7.7	1.27	Cadmium	12.2	102	3.18	2219-T87	406 × 406	Yes	7.2	—	—
4-1407	2.244	7.91	5.74	17.8	1.27	Cadmium	17.7	102	3.18	2219-T87	406 × 406	Yes	Petaled	130.6	415.5
4-1408	1.180	6.39	2.66	8.2	1.27	Cadmium	12.4	102	3.18	2219-T87	406 × 406	Yes	9.2	7.1	65.5
4-1409	0.804	5.62	3.37	10.4	1.27	Cadmium	13.2	102	3.18	2219-T87	406 × 406	Yes	6.4	0.1	—
4-1410	1.586	7.05	5.83	18.1	1.27	Cadmium	16.1	102	3.18	2219-T87	406 × 406	No	18.3	—	—
4-1411	0.970	5.98	2.45	7.6	1.27	Cadmium	11.4	102	3.18	2219-T87	406 × 406	No	4.7	—	—
4-1412	0.567	5.00	3.42	10.6	1.27	Cadmium	11.7	102	3.18	2219-T87	406 × 406	No	1.0	—	—
4-1413	1.878	7.46	5.78	17.9	1.27	Cadmium	17.5	102	3.18	2219-T87	406 × 406	No	23.2	—	—
4-1414w	1.872	7.45	5.78	17.9	1.27	Cadmium	17.2	102	3.18	2219-T87	375 × 375	Yes	Petaled	115.6	345.4
4-1415a	0.373	6.34	7.19	7.2	1.27	6061-T6	12.3	102	3.18	2219-T87	406 × 406	Yes	—	19.6	—
4-1416a	0.310	5.96	7.09	7.1	1.27	6061-T6	11.8	102	3.18	2219-T87	406 × 406	No	3.2	—	—
4-1417a	0.310	5.96	6.94	6.9	1.27	6061-T6	11.8	102	3.18	2219-T87	406 × 406	No	3.8	—	—
4-1418w	0.707	5.38	3.38	10.5	1.27	Cadmium	12.7	102	3.12	2219-T87	375 × 375	No	1.9	—	—
4-1419	1.171	6.37	4.85	15.0	1.27	Cadmium	14.7	102	3.18	2219-T87	406 × 406	Yes	13.8	5.8	—
4-1420	0.965	5.97	2.20	6.8	1.27	Cadmium	11.1	102	3.18	2219-T87	406 × 406	Yes	7.4	—	12.7
4-1421	0.784	5.57	4.36	13.5	1.27	Cadmium	14.0	102	3.18	2219-T87	406 × 406	No	7.6	—	—
4-1422	0.954	5.95	2.32	7.2	1.27	Cadmium	11.2	102	3.18	2219-T87	406 × 406	No	5.1	—	—
4-1424w	0.299	4.04	1.38	4.3	1.27	Cadmium	7.2	102	3.05	2219-T87	375 × 375	Yes	Warped	4.1	—
4-1423c	0.944	5.93	2.32	7.2	1.27	Cadmium	11.3	102	3.18	Cadmium	102 × 152	Yes	8.3	0.6	—
4-1436s	1.886	7.47	5.74	17.8	1.27	Cadmium	17.2	102	3.10	6061-T6	406 × 406	Yes	Petaled	85.9	197.4
4-1437t	1.884	7.46	5.62	17.4	1.27	Cadmium	17.7	102	2.29	2024-T3	406 × 406	Yes	Petaled	165.4	266.2
4-1439*	0.813	5.64	5.65	17.5	1.27	Cadmium	—	102	3.18	2219-T87	406 × 406	Yes	1.7	2.4	—
4-1440*	0.719	5.42	5.66	17.5	1.27	Cadmium	—	102	3.18	2219-T87	406 × 406	Yes	0.9	0.6	—
4-1445w	1.158	6.35	3.41	10.6	1.27	Cadmium	14.7	102	3.15	2219-T87	375 × 375	Yes	9.8	2.8	71.1
4-1446w	2.317	8.00	3.43	10.6	1.27	Cadmium	15.1	102	3.23	2219-T87	375 × 375	Yes	Petaled	51.3	116.6
4-1447t	1.912	7.50	5.67	17.6	1.27	Cadmium	18.2	102	3.25	2024-T3	406 × 406	Yes	Petaled	53.3	148.1
4-1438d	0.943	5.93	3.33	10.3	1.27	Cadmium	20.3	114	3.18	2219-T87	406 × 406	Yes	—	13.7	—
4-1401	1.130	6.29	5.01	15.5	1.49	Cadmium	17.4	203	3.18	2219-T87	406 × 406	No	1.0	—	—
4-1402t	1.165	6.36	5.54	17.2	1.49	Cadmium	17.0	203	1.60	2024-T3	381 × 381	No	15.9	—	—
4-1434d	2.223	7.89	3.56	11.0	1.27	Cadmium	10.7	305	4.06	6061-T6	406 × 406	Yes	—	25.9	—
4-1426s	1.167	6.36	5.49	17.0	0.53	Cadmium	10.6	356	1.27	6061-T6	381 × 381	No	27.1	—	—
4-1396	3.930	9.54	2.22	6.9	0.81	Cadmium	12.6	381	3.18	2219-T87	229 × 229	Yes	—	19.1	Holes
4-1397	3.939	9.54	2.59	8.0	0.81	Cadmium	12.9	381	3.18	2219-T87	229 × 229	Yes	—	17.8	Holes
4-1398	3.939	9.54	2.60	8.1	2.24	Cadmium	21.2	381	3.18	2219-T87	406 × 406	Yes	0.5	2.5	Holes
4-1425w	1.160	6.35	5.55	17.2	0.53	Cadmium	—	381	3.23	2219-T87	375 × 375	No	0.6	—	—
4-1427s	2.250	7.92	3.38	10.5	1.27	Cadmium	15.4	381	4.06	6061-T6	406 × 406	No	2.5	—	—
4-1430s	2.253	7.92	5.20	16.1	1.27	Cadmium	16.6	381	4.06	6061-T6	406 × 406	No	14.6	—	—
4-1431s	2.222	7.89	5.64	17.5	1.27	Cadmium	—	381	1.27	6061-T6	406 × 406	No	59.3	—	—
4-1432s	2.235	7.90	5.00	15.5	1.27	Cadmium	16.7	381	1.27	6061-T6	406 × 406	No	60.5	—	—
4-1442	0.936	5.91	5.98	18.5	0.97	Cadmium	13.1	381	3.18	2219-T87	406 × 406	No	1.9	—	—
4-1443	2.258	7.93	2.27	7.0	1.27	Cadmium	12.9	381	3.18	2219-T87	406 × 406	Yes	Warped	4.8	—
4-1444d	0.940	5.92	3.29	10.2	1.27	Cadmium	19.8	381	3.18	2219-T87	406 × 406	Yes	—	10.4	—
4-1448a	0.154	4.77	7.06	7.1	0.81	1100-O	9.6	381	1.75	6061-T6	305 × 305	Yes	Warped	5.1	—

Notes:
1) Shot number with an "a" suffix denotes aluminum projectile and aluminum bumper.
2) Shot number with a "c" suffix denotes rear wall was cadmium.
3) Shot number with a "d" suffix denotes projectile was a thin disk.
4) Shot number with a "s" suffix denotes rear wall was 6061-T6 aluminum.
5) Shot number with a "t" suffix denotes rear wall was 2024-T3 aluminum.
6) Shot number with a "w" suffix denotes a rear wall panel size of 375 mm square that was milled from a 25.4-mm thick plate 406 mm square leaving a 32-mm wide stiffener.
7) Shots numbered 4-1425w and 4-1431s had trailing sabot particles, which hit the hole in the bumper making hole size measurement unreliable.
8) Shots numbered 4-1439* and 4-1440* had impact angles of 54 deg. Trailing sabot particles made measurement of bumper hole size unreliable.

Results and Discussion

Ballistic Limit Curve

To validate the simulation method, several experiments were performed to compare the predicted ballistic limit curve for aluminum, based on cadmium simulations, with actual results for aluminum shields. In particular, six cadmium tests were conducted over a range of scaled velocities of 6 to 8 km/s (Fig. 4), four of which resulted in perforation of the wall. To compare these results with the aluminum shield they were designed to simulate, three experiments were conducted with aluminum impactors and bumpers (of the same dimensions as the cadmium). The velocity-scaled cadmium results provided an accurate prediction of the aluminum behavior. Both the aluminum and cadmium were perforated by impactors 6.35 mm in diameter and neither material was perforated by impactors 5.95 mm in diameter. An additional comparison is made in Fig. 4 with results from tests conducted at the Marshall Space Flight Center[18] (MSFC) and at the Johnson Space Center (JSC) Hypervelocity Impact Research Laboratory.[19] All of the experiments shown used common dimensions for bumper thickness, spacing, and wall thickness (however, MSFC used a wall thickness of 1.6 mm, rather than 1.27 mm). These data are all consistent with the cadmium results, with the exception of a single test from the Marshall data set that did not perforate.

Even though the ballistic-limit curves for cadmium and aluminum agree well near 7 km/s, there were some differences in the manner in which the wall was perforated. The aluminum tests exhibited some spallation on the back surface of the wall, whereas the cadmium tests did not. This is an artifact of the simulation method. For example, a cadmium test at a scaled velocity of 7 km/s is conducted at an actual velocity of 7/3.1 = 2.3 km/s. As a result, the velocities in the debris

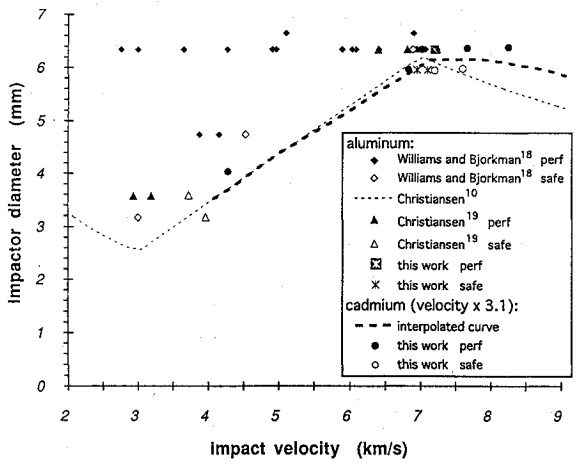

Fig. 4 Comparison of aluminum test results with cadmium simulations at scaled velocities near 7 km/s. The aluminum data in the melt regime are from Williams and Bjorkman,[18] Christiansen,[19] and this work. Note truncation of plot scales.

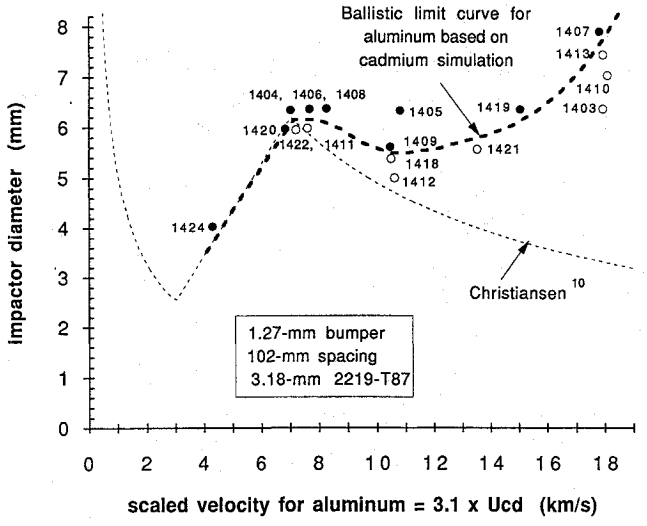

Fig. 5 Cadmium results for scaled velocities up to 18 km/s. These results show a ballistic-limit curve with an upward trend for velocities greater than about 10 km/s. This is in contrast to the behavior predicted by existing shield models, which show a monotonic decrease for velocities above 7 km/s.

cloud will be a factor of 3.1 lower than for an aluminum impact, while the time scale over which the debris is deposited on the wall is a factor of 3.1 longer. Therefore, while the cadmium test matches the impulse of the aluminum impact, the peak stress generated at the wall (which is related to the impact velocity, wave speed, and density) will be lower in the cadmium simulations. Therefore, cadmium might not provide an exact simulation at low velocities, where solid-particle impact causes spallation. However, note that shot 1424, at a scaled velocity of 4 km/s, is in good agreement with the aluminum results near 4 km/s.

Figure 5 shows the cadmium data set over the entire range of velocities tested, i.e., up to a scaled velocity of 18 km/s. Below about 10 km/s, the curve mimics the trend that most models have predicted for aluminum. That is, the minimum diameter for penetration increases with velocity until complete melting of the impactor and bumper material occurs (above 7 km/s for aluminum). Above this velocity, the curve turns downward. However, for velocities between 10 and 18 km/s, the diameter again increases with velocity. This is attributed to vaporization of the debris. In the 7- to 10-km/s range, much of the debris is expected to be in the form of very small molten droplets that may apply localized loadings and therefore may be relatively efficient penetrators (but less efficient than solid fragments). Above a scaled velocity of about 10 km/s, the debris cloud is largely vaporized and applies its loading uniformly over the area of contact with the wall. Therefore, as velocity increases and vaporization becomes more important, larger impactors are required to perforate the wall.

The increase in the ballistic-limit curve for velocities larger than 10 km/s is consistent with the cadmium experiments reported by Hopkins et al.[5] Those experiments used a constant impactor size, bumper thickness, and spacing, and varied the wall thickness to determine the minimum value required to prevent penetration as a function of impact velocity. As shown in Fig. 2, for scaled velocities above about 10.5 km/s, faster impactors were contained by thinner walls. That is, for a given impactor size, higher impact velocities presented less severe loadings on the wall.

Debris-Cloud Similarity

The previous section showed that the ballistic limit estimate for aluminum based on the cadmium simulations agreed well with the actual aluminum results. As an additional comparison, Fig. 6 shows the debris cloud from an aluminum shot and from a cadmium simulation. The left side of the figure shows the result of shot 1415a, an impact of a 6.35-mm-diam aluminum sphere on a 1.27-mm-thick aluminum bumper at 7.2 km/s. The right side of the figure shows the cloud from shot 1422, in which a 5.95-mm-diam cadmium sphere struck a 1.27-mm-thick cadmium bumper at an actual velocity of

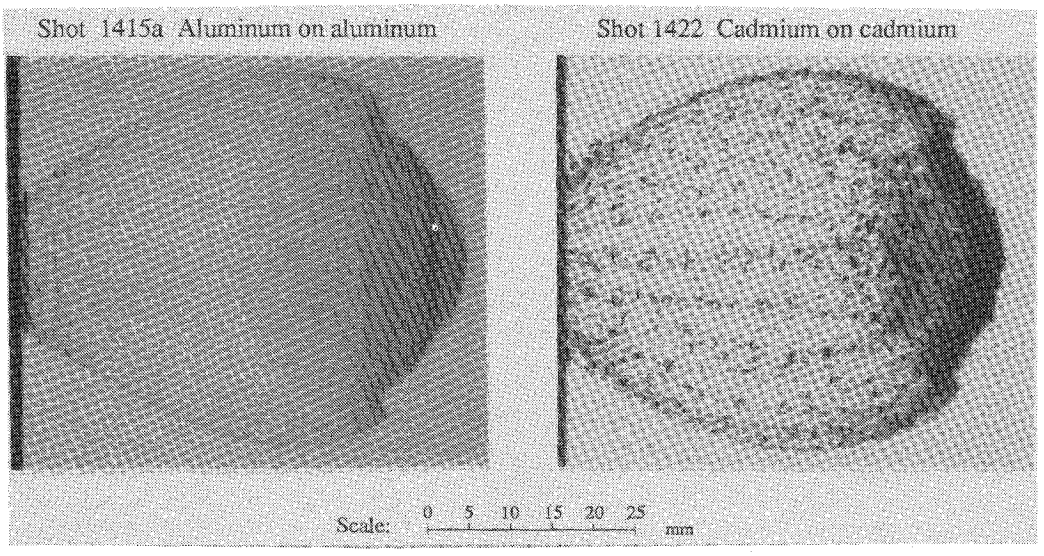

Fig. 6 The shape of the debris cloud produced by an aluminum projectile striking an aluminum bumper (shot 1415a, velocity = 7.2 km/s, diam = 6.34 mm) is matched quite well by a cadmium simulation (shot 1422, velocity = 2.32 km/s, diam = 5.95 mm).

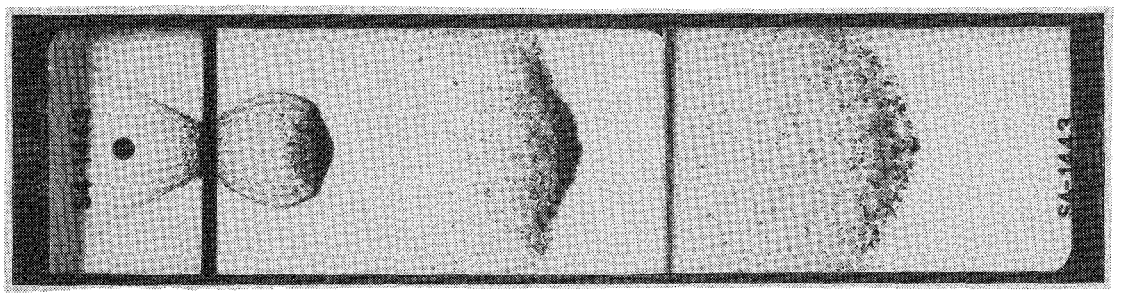

Fig. 7a Multiple exposure x-ray images of the debris cloud from shot 1443, an impact of a cadmium projectile onto a cadmium bumper at an equivalent velocity of 7.0 km/s (actual velocity of 2.27 km/s). At this velocity, the debris cloud contains an abundance of particles and/or droplets. Impactor diameter was 7.93 mm and bumper thickness was 1.27 mm.

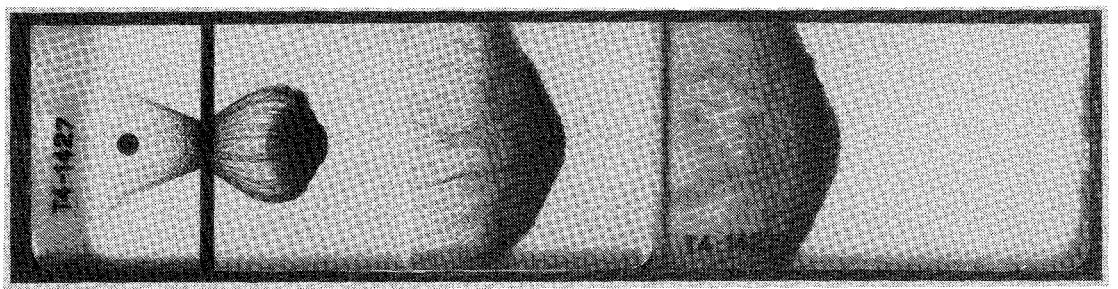

Fig. 7b Debris-cloud evolution from shot 1427s, which was at an aluminum-equivalent velocity of 10.5 km/s. Note that particles and/or droplets are less obvious here than in the lower-velocity test shown in Fig. 7a. Impactor diameter was 7.92 mm and bumper thickness was 1.27 mm.

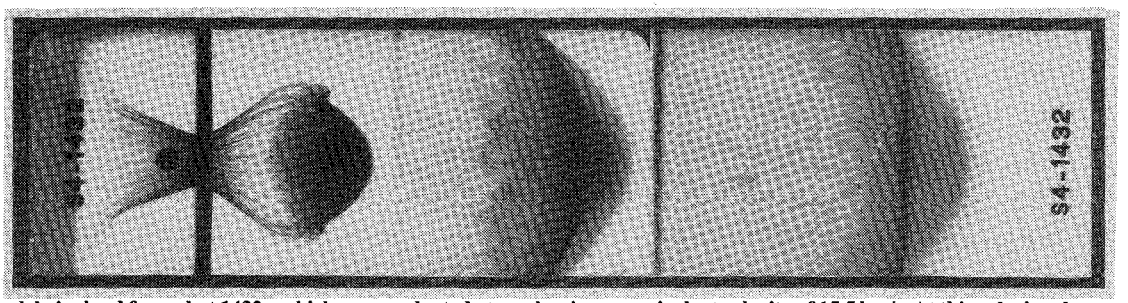

Fig. 7c The debris cloud from shot 1432s, which was conducted at an aluminum-equivalent velocity of 15.5 km/s. At this velocity, the particles, which characterized the shot at 7 km/s, are replaced by vaporized material. Impactor diameter was 7.90 mm and bumper thickness was 1.27 mm.

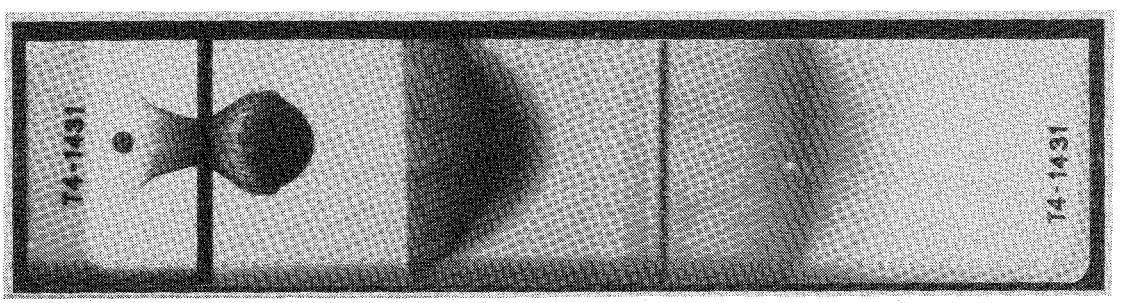

Fig. 7d The debris cloud from shot 1431s, which is similar to that shown in Fig. 7c above, except that the aluminum-equivalent velocity was 17.5 km/s. Impactor diameter was 7.89 mm and bumper thickness was 1.27mm.

2.32 km/s, i.e., a scaled velocity of 7.19 km/s. Although the impactor diameters differed slightly (7%), these two shots provide a good comparison of aluminum and cadmium at the same scaled velocity. Except for the region near the bumper, the overall shape of the cadmium cloud reproduced that of the aluminum quite well. On the other hand, the sizes of the fragments in the cadmium test appear to be larger than those for aluminum. It may be that cadmium is a more efficient absorber of x-rays, making fragments more visible in the image of the cadmium test. Alternatively, it may represent a slightly different fragmentation pattern or scaled strength. In this regard, it is interesting to note that shot 1448a, which used commercially pure aluminum (1100-O), showed somewhat larger fragments than comparable shots using the 2017-T4 aluminum alloy.

Figures 7a–7d are multiple-exposure radiographs showing debris-cloud growth from four cadmium simulations illustrating the effect of impact velocity on the cloud. In these tests, all parameters were held constant except for the scaled impact velocity, which ranged from 7.0 to 17.5 km/s. Note that finite particles and/or droplets are abundant in the cloud for 7 km/s (Fig. 7a), but are very much smaller in the cloud for the 10.5-km/s shot (Fig. 7b). In the higher-velocity shots (Figs. 7c and 7d), no particles are apparent. This is consistent with Fig. 5, which shows an upward turn in the ballistic limit curve near 10 km/s. That is, as the scaled velocity increases beyond 10 km/s, melting and vaporization of the particles reduces their penetration effectiveness. Therefore a larger impactor is required for perforation at 17 km/s than at 10 km/s.

Wall Perforation

Figures 8a–8d compare the walls for two tests at 7.2 km/s, which used aluminum impactors and bumpers, with the results of two cadmium simulations. The walls in all four tests were identical (3.18-mm-thick 2219-T87). Figure 8a shows the result of aluminum shot

1415a, in which the impactor was slightly above the ballistic limit. The perforation pattern was a single hole, roughly 20 mm in diameter. The cadmium simulation, shot 1404, also produced a perforation, with a hole of comparable linear dimensions (Fig. 8c). Figures 8b and 8d show aluminum and cadmium results with an impactor whose diameter was only 0.4 mm smaller than those in Figs. 8a and 8c. Neither of these smaller impactors perforated the walls, which leads to the following conclusions. First, the transition from no penetration to penetration is very sensitive to a small change in impactor size.

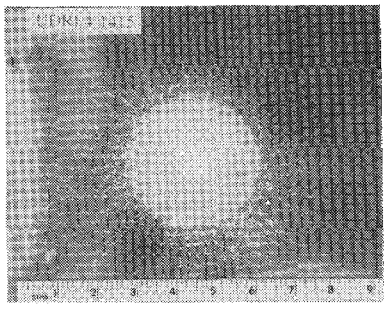

Fig. 8a Rear wall from shot 1415a at 7.2 km/s; 6.34-mm aluminum sphere perforated.

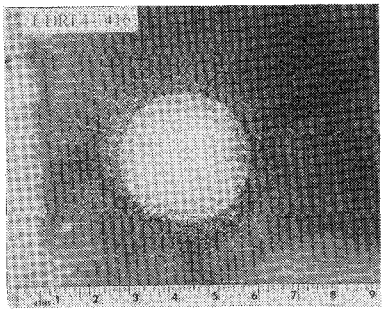

Fig. 8b Rear wall from shot 1416a at 7.1 km/s; 5.96-mm aluminum sphere did not perforate.

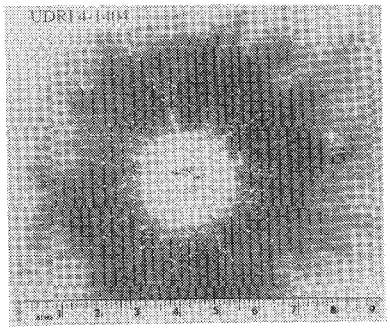

Fig. 8c Rear wall from shot 1404 at 7.0 km/s (scaled); 6.35-mm cadmium sphere perforated.

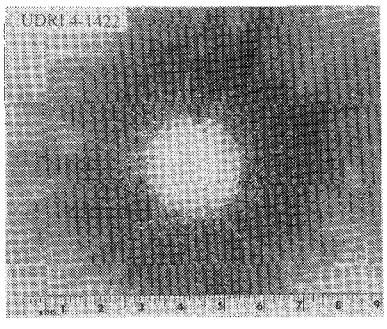

Fig. 8d Rear wall from shot 1422 at 7.2 km/s (scaled); 5.95-mm cadmium sphere did not perforate

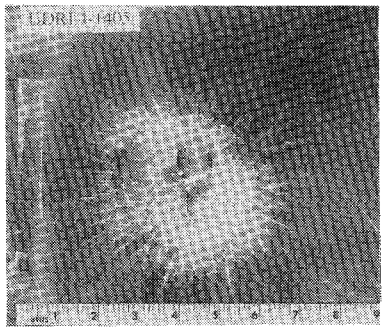

Fig. 9a Rear wall from shot 1405 at 10.8 km/s (scaled); 6.34-mm-diameter cadmium sphere perforated.

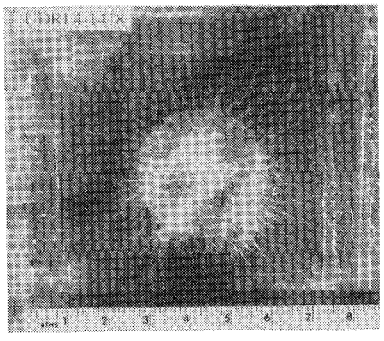

Fig. 9b Rear wall from shot 1418w at 10.5 km/s (scaled); 5.38-mm cadmium sphere did not perforate.

Second, the cadmium simulations reproduced the aluminum tests not only in the quantitative outcome of the event (i.e., perforation or no perforation), but also in the qualitative appearance of the debris character and pattern on the wall.

Figures 9a and 9b show the results of two cadmium tests at an equivalent velocity near 11 km/s. Figure 9a shows the front wall for shot 1405, which perforated. Note that at this velocity, in contrast to 7.2 km/s, the perforation consisted of a hole with radial cracks roughly 25 mm in length. Figure 9b shows the result of shot 1418w, which used a 15% smaller impactor diameter and consequently did not perforate the wall.

Figures 10a and 10b compare the walls from two cadmium simulations at an equivalent velocity near 18 km/s. Shot 1407 (Fig 10a) resulted in a severe failure of the wall with a hole roughly 100 by 150 mm and cracks 100 to 200 mm long, one of which extended across the plate. On reducing the impactor diameter slightly (6%) in shot 1413, the impactor did not perforate, but did produce a 25-mm bulge in the wall (Fig. 10b).

Effect of Wall Stiffeners

A few tests were conducted with walls that were milled from 25.4-mm-thick 2219-T87 plate to simulate a "waffle" structure with stiffeners at 406 mm centers. The plates were milled in such a way to leave a stiffener, 15.7 mm wide and 22.2 mm deep, around the perimeter of the plate. Impact tests near a scaled velocity of 18 km/s showed that stiffening a plate made it more susceptible to failure. In particular, the result of shot 1413, which used a nonstiffened plate, was a bulge 25 mm deep over a circular area about 100 mm in diameter, with no perforation. On the other hand, the stiffened plate used in shot 1414w (which was otherwise identical to 1413) ended up with a 110-mm-diam hole, severe petaling, and five radial cracks approximately 180 mm long. Note, however, that even though the outcomes differed dramatically, the stiffened plate may not affect the ballistic limit curve very much, because, as noted above, a small reduction in the impactor size in shot 1414w would result in no perforation of the wall.

Tests at a scaled velocity of 10.6 km/s showed very little difference between stiffened and unstiffened walls. For example, the unstiffened wall in shot 1405 was penetrated, with five radial cracks and a maximum tip-to-tip crack length of 71 mm. Shot 1445, a re-

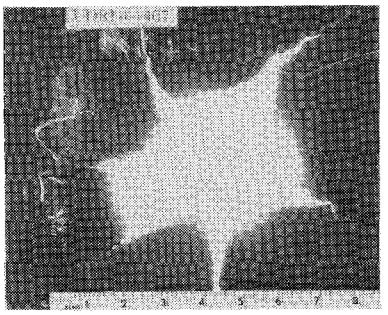

Fig. 10a Rear wall from shot 1407 at 17.8 km/s (scaled); 7.91-mm cadmium sphere perforated.

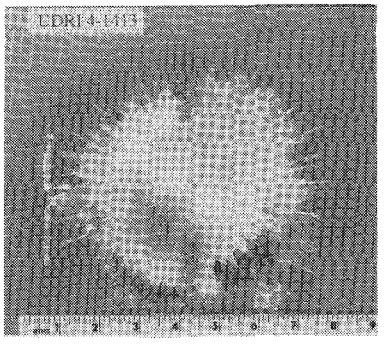

Fig. 10b Rear wall from shot 1413 at 17.9 km/s (scaled); 7.46-mm cadmium sphere did not perforate.

peat of 1405, but with a stiffened plate, showed a very similar type of failure.

Dispersion of the Debris Cloud

Models of debris-shield performance rely on assumptions regarding the geometry of the debris cloud as it propagates from the bumper to the wall. For example, Wilkinson[9] assumed that the angular dispersion of the cloud is independent of the impactor velocity. On the other hand, the model of Lawrence[22] predicts that cloud dispersion should increase as impact velocity increases. To date, there has been very little experimental evidence available to constrain these models in the melting and vaporization regimes. With these new data for cadmium, the cloud geometry and its dependence on impact velocity are now examined in detail.

To isolate the effects of velocity, a series of four shots were selected for analysis in which the scaled velocity ranged from 7.7 to 17.9 km/s. All other parameters were constant for this set of tests. Only a single x-ray image of the cloud was obtained in each shot, because of the wall placement 102 mm behind the bumper.

To compare the cloud shapes on an equal basis, it is necessary to capture the image of the cloud at a common stage of growth, such as the instant the leading edge contacts the wall, or when the cloud has expanded halfway to the wall. However, because of timing differences, the position of the cloud varied somewhat from one experiment to the next. Therefore, a method was developed to scale the cloud size to a common basis. After an examination of several shots for which multiple exposures were available, it was noted that cloud growth is very nearly isotropic. That is, if a cloud were imaged at two different times, and the earlier image was enlarged, it provided a good approximation to the cloud shape at the later time. As an example of this, Fig. 11a shows a triple exposure of a 1-g copper ball (6-mm diam) striking a 1.52-mm-thick copper bumper at 6.46 km/s.[16] An outline of the cloud from image 2 was drawn and then enlarged such that the leading edge of the outline corresponded with that of the cloud in image 3. Although some deviation occurs near the bumper (perhaps because of strength effects of the bumper at late times), the enlarged outline provides a very good prediction of the remainder of the cloud boundary.

Noting the apparent isotropic growth of the cloud, radiographs from the four selected cadmium experiments were digitized, trans-

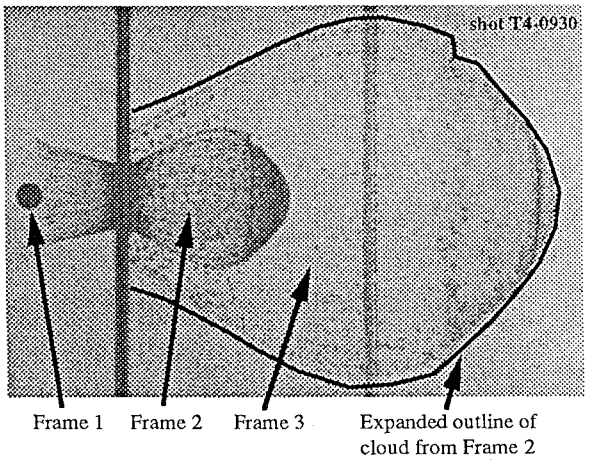

Fig. 11a Three x-ray images of an impactor just before striking a bumper at 6.46 km/s and the resulting debris cloud at two later times. The heavy line overlaid on image 3, obtained from an enlargement of image 2, shows that cloud shape did not change significantly with time.

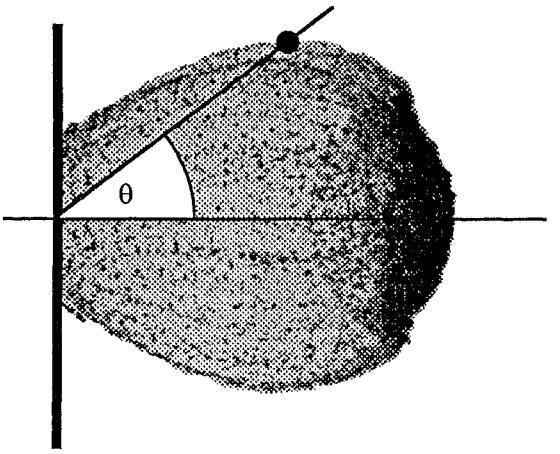

Fig. 11b Definition of cloud-dispersion angle.

ferred to an image-processing program on a computer, and enlarged or reduced so as to give them a common dimension as measured along the axis of impact. The final images are shown in Fig. 11c. While there are some notable differences in the cloud structure, the dispersion angle for each cloud (Fig. 11b) is quite insensitive to the impact velocity, with a value typically around 40 deg.

Impactor-Shape Effects and Comparison with HVL Data

The Sandia Hypervelocity Launcher (HVL) facility[23] provides an opportunity to directly compare and validate the cadmium simulation technique for velocities near 10 km/s, subject to certain assumptions concerning impactor geometry, integrity, and initial conditions. Ang et al.[20] and Hill et al.[21] report preliminary results for thin disks impacting various target geometries. The initial conditions used in the HVL tests differ from the nominal impactor shape and shield geometry used here. Consequently, four shots in the present study were allocated to provide a comparison between cadmium simulations and the HVL tests. The results of the simulations, along with those reported by Ang et al. and Hill et al. are listed in Table 2 and shown in Fig. 12.

Shot 1438d was a direct simulation of Hill-1, i.e., the cadmium disk in 1438d had the same dimensions as the aluminum disk in Hill-1, but an actual impact velocity that was a factor of 3.1 lower. However, 1438d perforated the wall, whereas Hill-1 did not.

To obtain more information on these differing outcomes, shot 1444d was set up as a repeat of 1438d, except the bumper spacing was increased to 381 mm so that two additional x-ray images could be obtained. As can be seen on the far left of Fig. 13a, the disk impacted flat, to within measurement capability. The radiographs

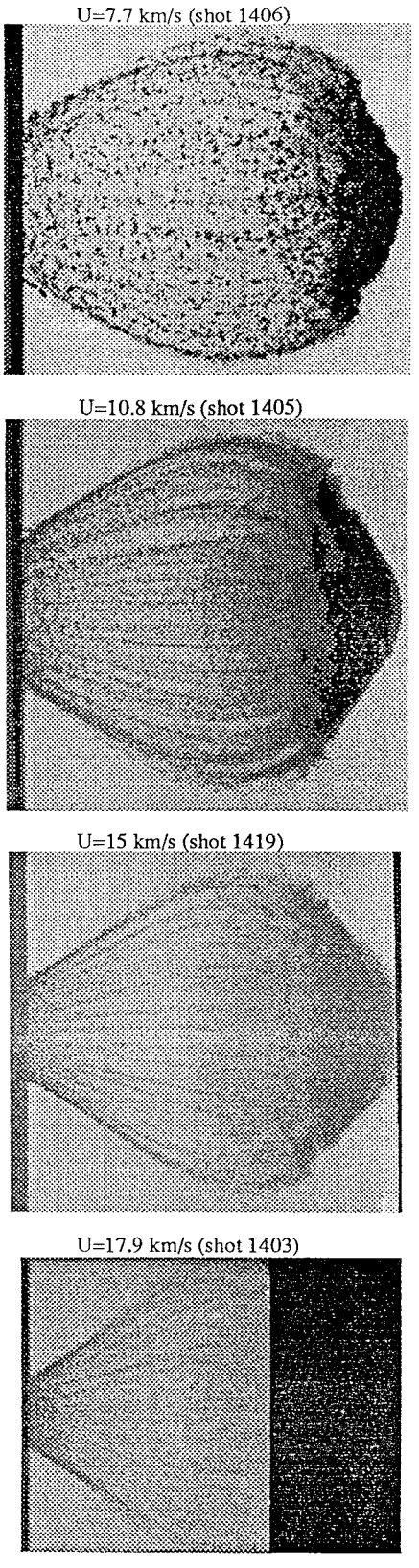

Fig. 11c Tests with cadmium bumpers and impactors show that the cloud-dispersion angle is about 38 deg to 40 deg for all of the scaled impact velocities shown.

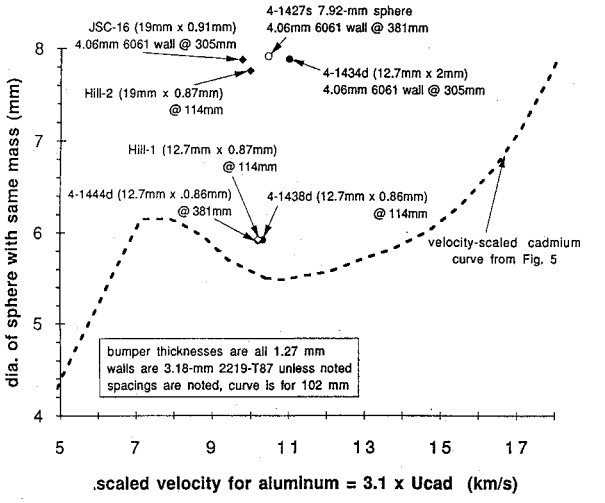

Fig. 12 Comparison of thin-disk cadmium results with those for aluminum disks launched in the Sandia HVL from Ang et al.[20] and Hill et al.[21]

also show what appears to be a dense core following the front. The original disk, 0.86 mm thick, impacted a bumper that was 1.27 mm thick. This creates a condition where a piece of the bumper, almost identical in shape to the impacting disk, spalls off with approximately the impact velocity and strikes the wall as though the bumper were not even there. The remaining thickness of the bumper and the original impactor decelerate because of stress-wave interactions that are nearly one-dimensional in nature, resulting in a velocity distribution that decays spatially nearly linearly to zero on the upstream side of the impacting disk. This produces what appears to be a porous, rodlike debris cloud with little spatial dispersion and therefore great damage potential.

The above discussion implies that Whipple bumpers are ineffective against disks impacting flat. To demonstrate this, Fig. 13b shows that the disk in shot 1444d perforated the wall at a spacing of 381 mm with almost the same intensity as it did at a spacing of 114 mm in shot 1438d (Fig. 13c). The diameter of the hole in the wall was approximately 57% larger than the disk diameter for both shots, consistent with the observation of minimal radial dispersion of the debris cloud. In contrast, consider the impact of the sphere in shot 1427s. A slightly thicker wall (of 6061-T6) was used for this shot than for 1444d, and an impactor mass that was 240% larger. Yet the spherical impactor barely scuffed the wall. This is due to the much greater radial expansion of the debris cloud for spherical impactors (Fig. 7b) than for disks impacting flat.

Because no preimpact radiographs or photographs are available for the Hill-1 shot, we speculate that the impactor in that test may not have presented the severe, planar type of loading exhibited by 1438d and 1444d. Partial support for this speculation is given by the x-ray image in Fig. 2 of Ang et al.[20] that shows, for a "typical intact flyer plate launch," a disk that is bowed and rotated prior to striking the bumper. It seems likely that shot Hill-1 did not produce a rodlike debris cloud like the one shown in Fig. 13a and therefore would have been less likely to perforate than shot 1438d.

The 19.0-mm-diam disks in shots JSC16 and Hill-2 could not be accommodated in the particular UDRI gun used for the present study. As an approximate simulation of JSC16, shot 1434d used a disk that simulates the same mass as JSC16, but has a smaller diameter and larger thickness (12.7 by 2.0 mm). As a result, the diameter/thickness ratio was 6 for the cadmium simulation and 21 for the HVL test. Four-exposure x-ray images of 1434d show the disk flying nearly edge on (as opposed to flat) as it impacts the bumper. The resulting debris cloud perforated the wall, which is consistent with the perforation reported for JSC16.

A comparison between spherical impactors and disks can be made by comparing JSC16 with shot 1427s, a cadmium simulation of a spherical aluminum impactor with the same mass as the disk used in JSC16. An additional comparison can be made between 1427s and 1434d, whose impactors had the same mass, but differing geometries. As mentioned above, the four-image radiographs for shot 1427s in Fig. 7b show considerable radial dispersion in the debris cloud, thereby mitigating the loading on the wall. As a result, 1427s did not perforate, while both of the disk shots JSC16 and 1434d did.

The HVL shot, Hill-2, resulted in a perforation, which is not surprising, because it used a similar disk size and velocity to JSC16,

Table 2 Summary of disk impact data for cadmium and from Sandia HVL for aluminum (Refs. 20, 21)

Shot number	Mass m, g	Disk diam d_{cyl}, mm	Thickness h, mm	Projectile material	Velocity U, km/s	Diam d, mm	Bumper Thickness b, mm	Bumper material	Spacing S, mm	Wall thickness t, mm	Wall material	Failure
1427s	2.250	—	—	Cadmium	10.50	7.92	1.27	Cadmium	102	4.06	2219-T87	No
1434d	2.223	12.7	2.03	Cadmium	11.00	7.89	1.27	Cadmium	305	4.06	2219-T87	Yes
1438d	0.943	12.7	0.86	Cadmium	10.30	5.93	1.27	Cadmium	114	1.27	2219-T87	Yes
1444d	0.940	12.7	0.86	Cadmium	10.20	5.92	1.27	Cadmium	381	1.27	2219-T87	Yes
Hill-1	0.295	12.7	0.87	6061-T6	10.20	5.93	1.27	6061-T6	114	3.18	2219-T87	No
Hill-2	0.661	19.0	0.87	6061-T6	10.00	7.76	1.27	6061-T6	114	3.18	2219-T87	Yes
Hill-3	1.498	28.6	0.87	6061-T6	10.30	10.19	1.27	6061-T6	114	3.18	2219-T87	Yes
JSC5	0.793	19.0	1.03	6061-T6	7.19	8.25	1.27	6061-T6	305	4.05	6061-T6	No
JSC16	0.692	19.0	0.90	6061-T6	9.80	7.88	1.27	6061-T6	305	4.05	6061-T6	Yes

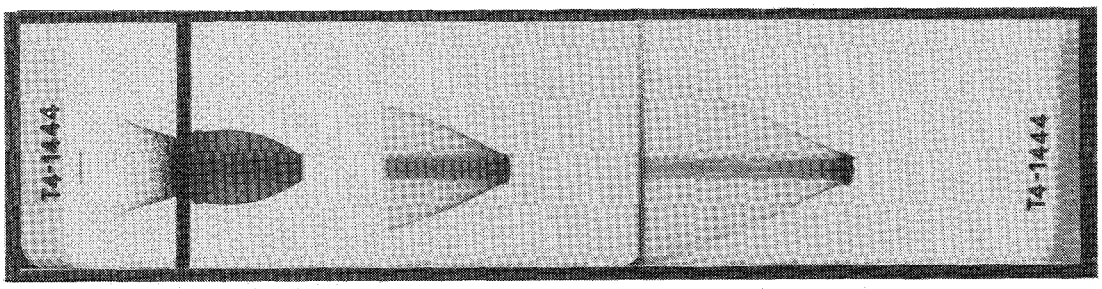

Fig. 13a The debris cloud from shot 1444d, a cadmium disk 12.7 mm in diam. and 0.86 mm thick impacting a 1.27-mm cadmium bumper with an aluminum-equivalent velocity of 10.2 km/s. The debris cloud shows a "porous rod like" structure with little radial dispersion, in marked contrast to spherical impactors.

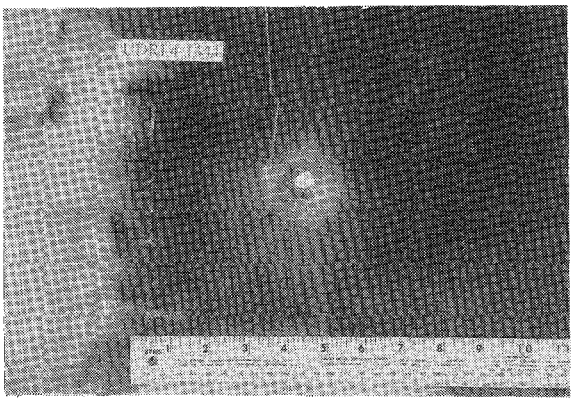

Fig. 13b The rear wall in shot 1444d was perforated, with a hole whose diameter is 55% greater than that of the impacting disk. This confirms the absence of radial dispersion of the cloud front.

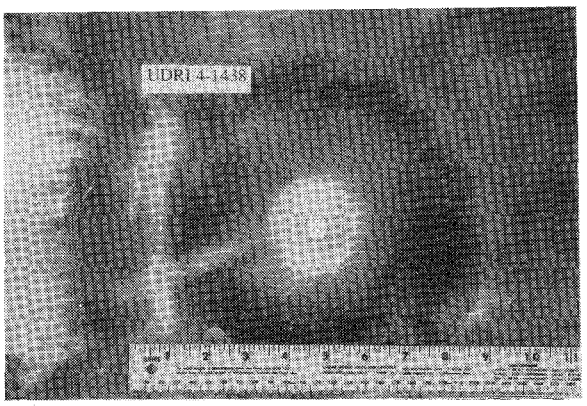

Fig. 13c Comparison of this photograph for shot 1438d (bumper spacing = 114 mm) with Fig. 13b (spacing = 381 mm) shows that increases in bumper spacing do little to prevent perforation for disk-shaped impactors.

but a smaller bumper spacing and wall thickness. A comparison of Hill-2 to either of JSC16 or 1427s reinforces the above conclusion that an increase in bumper spacing does little to mitigate the debris cloud formed by disk-shaped impactors.

Hill-3 also resulted in a perforation, which is expected because it used an even more massive disk than Hill-2. The final shot to be considered, JSC5, is an enigma, because it did not perforate even though it was more massive than JSC16, which did perforate. No cadmium disk simulations were performed at the velocity of JSC5 (7 km/s). However, note that the HVL produces considerable heating of the projectile, almost to the threshold of melting, during launch. This could increase the amount of melting and could drive it toward partial vaporization upon impact at this velocity. Again, without preimpact radiographs, a distortion or rotation of the impacting disk could cause radial expansion of the debris cloud, resulting in no perforation.

Conclusions

1) Scaling requirements are identified for the use of surrogate materials in simulating high-velocity impacts on aluminum debris shields. In the simulation method used here, an aluminum impactor and bumper are replaced by cadmium counterparts of the same dimensions. The important feature of this technique is that the response of aluminum at a velocity U is simulated with cadmium at a reduced impact velocity of $U/3.1$.

2) Cadmium was chosen because of its special material properties. Its density and specific heats of melt and vaporization allow a unique match of the actual initial momentum of an aluminum-on-aluminum impact while maintaining a constant shield geometry.

3) The scaling analysis shows that a cadmium surrogate, in addition to matching the initial momentum of an aluminum impactor, also matches the impulse transferred to the wall. This conclusion is supported by the experimental results of Mullin et al.,[7] in which the momentum transferred to the wall was measured for impacts of both aluminum on aluminum and cadmium on cadmium.

4) Test results for aluminum impactors and bumpers at 7 km/s show very good agreement with cadmium simulations at the same scaled velocity. These results, together with the generally good correspondence between the observed cloud shapes for the two cases,

validate the use of cadmium as a surrogate material in simulating the response of an aluminum shield.

5) Cadmium experiments at scaled velocities of 10 to 18 km/s show that the minimum impactor size for perforation of the wall increases with velocity, in sharp contrast to the typical behavior predicted by existing shield models. This behavior is believed to be the result of vaporization effects, which cannot be achieved using conventional testing methods on aluminum shields. At velocities above 10 km/s, vaporization of any fragments or melt droplets in the debris cloud tends to smooth their loading over a larger area on the wall, thereby reducing their perforation effectiveness.

6) The manner in which wall perforation occurred was found to depend on impact velocity. For slow impacts (equivalent to 7 km/s and below for aluminum), perforation was usually the result of a few small holes or cracks, with little structural deformation of the wall. On the other hand, at larger velocities, impactors somewhat below the minimum size for perforation produced substantial bulging of the wall. A slight increase in the impactor size resulted in failures typified by severe tearing and petaling of the wall.

7) Observations of the debris-cloud shape for spherical impactors are used to show that the cloud expands nearly isotropically as it moves toward the wall. The radial dispersion of the cloud is shown to be insensitive to changes in the impact velocity—an observation that could be incorporated into models of cloud evolution.

8) Cadmium tests show that a disk impacting flat against a bumper produces a rod-shaped debris cloud that exhibits very little radial dispersion with distance and therefore has great damage potential. Limited comparisons of cadmium disks launched at an aluminum equivalent velocity of 10 km/s show general agreement with the aluminum results from the Sandia Hypervelocity Launcher (HVL). Some discrepancies are noted but are believed to be due to the bowed and rotated state of the impactor in the HVL tests.

Acknowledgments

This research was supported by Boeing Defense & Space Group Independent Research and Development funds. Useful discussions with Keith Holsapple and the thoughtful comments of two anonymous reviewers are appreciated.

References

[1]Kessler, D. J., Reynolds, R. C., and Anz-Meador, P. D., "Orbital Debris Environment for Spacecraft Designed to Operate in Low Earth Orbit," NASA TM-100-471, April 1988.

[2]Maiden, C. J., and McMillan, A. R., "An Investigation of the Protection Afforded a Spacecraft by a Thin Shield," *AIAA Journal*, Vol. 2, No. 11, 1964, pp. 1992–1998.

[3]Swift, H. F., Preonas, D. D., Turpin, W. C., and Cunningham, J. H., "Characterization of Debris Clouds behind Impacted Meteoroid Bumper Plates," AIAA Paper 69-380, 1969.

[4]Gehring, J. W., "Theory of Impaction Thin Targets and Shields and Correlation with Experiment," *High Velocity Impact Phenomena*, edited by R. Kinslow, Academic Press, New York, 1970, pp. 105–155, 463–514.

[5]Hopkins, A. K., Lee, T. W., and Swift, H. F., "Material Phase Transformation Effects upon the Performance of Spaced Bumper Systems," *Journal of Spacecraft and Rockets*, Vol. 9, No. 5, 1972, pp. 342–345.

[6]Westine, P. S., and Mullin, S. A., "Scale Modeling of Hypervelocity Impact," *International Journal of Impact Engineering*, Vol. 5, No. 1–4, 1987, pp. 693–701.

[7]Mullin, S. A., Anderson, C. E., Jr., and Wilbeck, J. S., "Dissimilar Material Scaling Relationships for Hypervelocity Impact," Defense Nuclear Agency, Report DNA-TR-89-112, Washington, DC, 1989.

[8]Madden, R.,"Ballistic Limit of Double-Walled Meteoroid Bumper Systems," NASA TN D-3916, 1967.

[9]Wilkinson, J. P. D., "A Penetration Criterion for Double-Walled Structures Subject to Meteoroid Impact," *AIAA Journal*, Vol. 7, No. 10, 1969, pp. 1937–1943.

[10]Christiansen, E. L., "Design and Performance Equations for Advanced Meteoroid and Debris Shields," *International Journal of Impact Engineering*, Vol. 14, No. 1–4, 1993, pp. 145–156.

[11]Swift, H. F., Preonas, D. D., Dueweke, P. W., and Bertke, R. S., "Response of Materials to Impulsive Loading," Air Force Materials Lab., Report AFML-TR-70-135 (UDRI-TR-70-18/AD 783 315), Wright-Patterson AFB, OH, 1970.

[12]Holsapple, K. A., "Hypervelocity Impacts: Testing in Surrogate Materials," *International Journal of Impact Engineering*, Vol. 14, No. 1–4, 1993, pp. 335–345.

[13]Anon., *Alcoa Aluminum Handbook*, Aluminum Company of America, Pittsburgh, PA, 1962.

[14]Anon., *Metals Handbook*,Vol. 1, American Society for Metals, Metals Park, OH, 1969.

[15]Piekutowski, A. J.,"Debris Clouds Generated by Hypervelocity Impact of Cylindrical Projectiles with Thin Aluminum Plates, *International Journal of Impact Engineering*, Vol. 5, No. 1–4, 1987, pp. 509–518.

[16]Piekutowski, A. J., "A Simple Dynamic Model for the Formation of Debris Clouds," *International Journal of Impact Engineering*," Vol. 10, No. 1–4, 1990, pp. 453–471.

[17]Piekutowski, A. J., Characteristics of Debris Clouds Produced by Hypervelocity Impact of Aluminum Spheres with Thin Aluminum Plates, *International Journal of Impact Engineering*, Vol. 14, No. 1–4, 1993, pp. 573–586.

[18]Williams, R. R., and Bjorkman, M. D., "Results of Ballistic Limit Testing of Aluminum Meteoroid/Debris Shields," Boeing Document D683-10578-1, Contract NAS8-50000, Boeing Co., Huntsville, AL, 1992.

[19]Christiansen, E. L.,"Whipple Shield Sizing Equations," JSC Memo SN3-91-19, Johnson Space Center, Houston, TX, Dec. 18, 1990.

[20]Ang, J. A., Chhabildas, L. C., Cour-Palais, B. G., Christiansen, E. L., and Crews, J. L., "Evaluation of Whipple Bumper Shields at 7 and 10 km/s," AIAA Paper 92-1590, 1992.

[21]Hill S. A., Chhabildas, L. C., and Hertel, E. S., "A Comparison of Whipple Shield Hypervelocity Impact Tests to Penetration Predictors," work performed under NASA contract H-99071B, Marshall Space Flight Center Huntsville, AL, 1991.

[22]Lawrence, R. J.,"A Simple Approach for the Design and Optimization of Stand-off Hypervelocity Particle Shields," AIAA Paper 92-1465, 1992.

[23]Chhabildas, L. C., "A New Hypervelocity Launcher (HVL) for Space Science Application," AIAA Paper 92-1639, 1992.